8-2024

Bioaffinity analysis of aptamer-target interactions

Pooja Karunanithi
jsp833@mocs.utc.edu

Bioaffinity Analysis of Aptamer-Target Interactions

Pooja Karunanithi

Departmental Honors Thesis

The University of Tennessee at Chattanooga

Department of Computer Science and Engineering

Examination date: August 8th, 2024

Thesis Committee:

Bradley Harris

Director of Chemical Engineering

Thesis Director

YingFeng Yang

Assistant Professor in Computer Science

Committee Member

Michael Danquah

Professor and Associate Dean for Academic and Student Affairs

Committee Member

Table of Contents

I. Introduction

In the Spring of 2020, just a few months before the end of the school year, a novel virus that had been spreading across Asia and Europe finally reached the United States. Fear became reality as businesses and schools prepared to shut down for two weeks to “stop the spread”. Unfortunately, this novel coronavirus would continue to spread across the world, leading to a pandemic that raged for nearly two years and altered the global landscape perhaps irreparably.

Coronavirus is a type of single-stranded positive RNA virus with the largest known genome size, being 30 to 32 kilobases [1]. Within the coronavirus family, there are four different groups: alpha, beta, gamma, and delta. The alpha and beta virus only infect mammals while the other two viruses mainly infect birds and a few mammals [2]. There is a certain strain, called the severe acute respiratory syndrome coronavirus (SARS-CoV), that first caused an epidemic in 2002. While most coronavirus infections cause the common cold, SARS-CoV infections typically starts with a fever followed by respiratory signs and symptoms and potentially rapid respiratory failure. The reason SARS became an epidemic so quickly was because of its fast ability to spread. Transmission occurred primarily through respiratory droplets in a close distance. Other ways of transmission include direct or indirect contact with feces, animal vectors, or other respiratory secretions [5].

The first case of SARS-CoV was in Guangdong Province, China in November 2002. Animal handlers from Guangzhou city were one of the first people to contract SARS. It was suggested that civets were an intermediate host for SARS allowing it to enhance its infectivity. Then on February 21, 2003, a medical professor from the Guangdong Province was infected and traveled to Hong Kong. There he spread it to 2 family members, 4 health care workers, and 12 other residents making him a “super-spreader”. The transmission to the health care workers resulted in

SARS being spread to 32 different countries with 8422 cases and 919 deaths. One way of spreading in the hospital was through health care workers in the hospital not realizing that a person was infected with SARS. Consequently, this related to the infection of the health care workers, other patients, and the patients close contacts [5]. In April 2003, Beijing was getting around 173 new cases every day [3]. Beijing then produced different protocols that the citizens should follow to reduce the number of cases. These protocols included larger quantities of PPE and covid training for the front-line workers, establishment of more than 100 different fever clinics, designated hospitals for covid patients only, isolation of infected people, and accurate and timely reporting of cases. With these controlled measures, Beijing was able to eradicate the virus by June 20, 2003 [4].

SARS-CoV-2 (SARS2) is a novel type of coronavirus that is currently fueling a pandemic in the 21st century. According to data from Johns Hopkins University, there have been 676,609,955 global cases and 6,881,955 global deaths between January 22, 2020, through March 10,2023 [10]. Bats were confirmed to be the original source of SARS2 [6]. Studies have shown that the SARS2 genome is around 96% identical to the bat virus thus solidifying its origin. Moreover, evidence suggests that minks and pangolins could be some intermediate hosts of this virus [7]. The main route of transmission of this virus is through respiratory droplets from patients with pneumonia from SARS2. Additionally, there were confirmed cases of the novel coronavirus in the feces of patients in Wuhan. These cases show that there is possibility of fecal-oral transmission, and that the virus can exist and replicate in the digestive tract [7]. People with SARS2 can be asymptomatic meaning that the infected person will show no signs that they have the virus. On the other hand, people could be symptomatic by having fever, cough, and most commonly severe pneumonia. Some uncommon symptoms include headache, hemoptysis,

sputum, and diarrhea [7]. Newborns can also be infected with SARS2 from mother-to-child transmission. There was a case in Wuhan of a newborn testing positive from throat swabs just 30 hours after birth [7]. SARS2 typically infects people between ages 30-69 and the infection rate of children is relatively low but not impossible [8]. Since SARS2 has a quick transmission rate and can impact people of all ages around the world, the compositions and intricacies of the virus must be understood.

II. Literature Review

As mentioned above, coronavirus is an enveloped, positive, single-stranded RNA virus. This means that its viral genome is in the 5' to 3' direction and it can be directly translated into mRNA. After replication, its genome is translated into two polyproteins which are then subsequently cleaved into 7 different genes. The first gene on the polyprotein codes for non-structural proteins that are involved in the replication and transcription process. The rest of the genes code for the structural proteins that are involved in viral assembly, entry, and act as good targets for diagnosis [11]. On the virus envelope, there are the envelope (E), spike (S), membrane (M), and sometimes the hemagglutinin-esterase (HE) proteins and in the envelope is the nucleocapsid (N) protein [8]. The E protein's main function is the envelope formation and its stability while the S protein has a range of functions that include receptor binding, viral entry, fusion, host range, and more. S protein will recognize and target some of the host receptor and this will lead to viral fusion and entry [13]. The HE protein helps with viral entry, pathogenesis, and viral release [11]. However, not every strain of coronavirus has the HE protein present as a result of continuous mutations in the HE domain [12]. The M protein will contact both the S and N proteins that are required for the virion, the fully mature virus, formation. Finally, the N protein plays a role in forming helical nucleocapsid with the RNA genome and its interaction

with the M protein could result in an icosahedral shell [11, 14]. The N protein is made up of two different terminal domains, N (NTD) and C (CTD), which contain a serine-rich linker between them. NTD forms orthorhombic crystals that will bind to the genome and CTD promotes nucleocapsid formation along with forming stable dimers in solution [13]. Additionally, the N protein is the most abundant protein and is expressed during the early stages of infection meaning is it a good protein to use for targeting the virus [13]. The most common method for treating viral infections is the use of antiviral medicines which inhibit viral functions such as viral attachment, entry, uncoating, viral transcriptase, and more [28]. For SARS2 specifically, there are three different types of medication that can be taken which will stop viral replication [29]. Another way to stop viral infections is through convalescent plasma therapy. This is where the plasma from a previously infected person is used to collect the antibodies from the virus [30]. The antibodies are then used to target the viral cells and neutralize them. The mutation rate of viruses is high which causes a lack of effectiveness in the current forms of infection inhibition. Since SARS2 is a single-stranded RNA virus, it is more susceptible to mutations as compared to other double-stranded or DNA viruses [15]. These mutations cause different strains and pathogenicity. Mutations in the non-structural proteins (nsp) 2 and 3 of SARS2 is a possibility of its uniqueness to the 2002 SARS strain [13]. Some of the more novel ideas are protein targeted degradation using proteolysis-targeting chimera (PROTAC) and aptamers. PROTAC uses the E3 ubiquitin ligase and links it to the protein on interest which will promote degradation of the target [31]. E3 ligase is from the ubiquitin proteasome pathway which helps cells degrade proteins and recycle their amino acids [32].

In this project, aptamers will be used to target the N protein in the SARS2 virus. Aptamers are short sequences of nucleic acids, or oligonucleotides, which can have high binding affinity to a

specific target. The word aptamer is derived from the Latin work *Aptus*, meaning “to fit”. This word was chosen as it best described the lock and key relationship an aptamer can have with its target [16]. Aptamers have several unique qualities that make them better candidates for more advanced research as compared to the traditional way of fighting viral infections such as antiviral medication, PROTAC, and more. These include: (1) high stability meaning it will still function properly after being denatured and renatured, (2) aptamer production is easy and cheap, (3) the human body does not thing that aptamers are foreign agents so there is low immunogenicity, (4) targets can range from proteins, cells, drugs, metal ions, etc. [19]. Aptamers can be artificially engineered to target specific molecules through a process called systematic evolution of ligands by exponential enrichment (SELEX). In this process, a single-stranded nucleic acid, which is around 30 – 100 nt long, is incubated with the target molecule. During the incubation period, parts of the single stranded nucleic acid sequence will bind together and with the target [17]. Then the unbounded nucleic acid sequences are flushed out with a binding buffer solution while the bounded ones stay. Heat or several elution buffer washings will then be used to remove the nucleic acid sequences that are bound to the target. Using polymerase chain reaction (PCR), those sequences are amplified and ready to start the next round of the selection process. These steps are repeated for around 8 – 15 rounds and it will result in the aptamer candidate. Additionally, the binding affinity of the potential aptamer sequences and the target molecule will increase each round [18].

a. Surface Plasmon Resonance

Surface plasmon resonance (SPR) is a biosensing method that was developed in the early 1990s. It can be used to find the specificity, affinity, and kinetics of different types of bound complexes [21]. The SPR machines have three core components that

work by measuring the changes in a refractive index at a certain angle as a result of biomolecular interactions. These components are the sensor chip, the microfluidic system, and the detection units. The sensor chip is typically coated in a thin layer of gold and for some SPR machines the sensor is also coated in dextran matrix. Once this is finished, the sensor chip is placed inside the machine where it is primed with a buffer solution. After this, a solution with the ligand will be sent through the machine. The matrix will act as a substrate and the ligand will attach to them through covalent coupling. This attachment will create a hydrophilic environment that will be used for the interaction between the molecules and their receptor. Finally, the receptor is injected into solution where it will attach to the ligand that is on the sensor chip. Each receptor-ligand complex that occurs in the machine will alter the refractive index near the surface and the angle of the reflected intensity. This results in a proportional relationship between the amount of molecule bound and the change in the SPR angle [22].

b. Aptamer Binding Analysis

The aptamer-protein binding affinity can be studied through energy charts and Root Means Squared Deviation (RMSD) charts. Through energy charts, the amount of potential energy in a complex at different time steps can be measured. From there, the stability of one complex can be determined and compared to other complexes. A phenomenon called bond energy can also be related to its stability. Bond energy, which is the amount of energy necessary to break a bond, is directly related to its stability. Therefore, higher bond energy indicates a stronger bond meaning it requires more energy to break a bond. Another way to test the bond strength is through its

potential energy which is the measurement of energy that is in a complex based on its arrangement of atoms and bonds. Potential energy is inversely proportional to the bond energy therefore less potential energy means more stable binding.

Root Mean Squared Deviation (RMSD) charts are the averages of the distance between the backbone of a complex and its superimposed proteins or nucleic acids. These charts can show the stability of a complex by plotting the RMSD value against time. If the charts show very little fluctuation and an overall low RMSD value, it means that the complex is stable and has good binding affinity.

III. Methodology

a. Running the SPR structure machine

The first step in performing SPR analysis of aptamer-protein interaction is to immobilize the aptamer onto a sensor surface. This can be achieved by covalently linking the aptamer to a sensor chip through a linker molecule. The sensor chip is then placed in a SPR instrument, which allows for the detection of changes in the refractive index at the surface of the chip. The protein of interest is then flowed over the aptamer-modified chip, and any binding events between the protein and aptamer will result in a change in the refractive index, which can be detected in real-time by the SPR instrument. By measuring the binding kinetics of the aptamer-protein interaction, valuable information about the stability of the interaction can be obtained.

b. Selection of aptamer-protein complex

The specific aptamer that was used for this project has a sequence of: 5’ – gggcccgguagggcccggucgggccccggg -3’. This aptamer was obtained from Sabbih’s paper and was extracted through the SELEX process [20]. Sabbih used an oligonucleotide library from Yaroslav

et al, to design an aptamer that has an increased binding affinity with the N-protein [20, 23]. Sabbih used a minimum free energy of -5 $kcal.mol^{-1}$ and the parameter and its binding properties were found using RPISeq [20]. RPISeq will use random forests (RF) and support vector machines (SVM) to predict RNA and protein interactions using sequencing information [24]. RF are made up of several hundreds of decision trees. Each decision tree is unique through random sampling of data and parameters. The output of the RF is an average output of the decision trees [26]. On the other hand, support vector machines use a N-dimensional space to create a division between samples based on specified parameters [27].

The specific N-protein that was used has a code of 6M3M in the protein data bank (PDB). This molecule is the crystal structure of SARS-CoV-2 nucleocapsid protein N-terminal RNA binding domain. This structure was determined using X-ray diffraction and it has identified a unique potential RNA-binding pocket that will guide some antiviral drugs that can target SARS.

c. Preparing the complex for the simulation

Using a website called Hdock, the aptamer and aptamer will be “docked” 10 different ways. The “docking” process is created by binding the protein and aptamer complex in different conformations. Once the binding is completed, another website called charmm-gui.org is used to input the complex into a water box solution. It is necessary to put the aptamer-protein complex in a water box solution as it allows it to stabilize.

d. Running and visualization of simulations

Once the water box was created, computers at the MDR building at the University of Tennessee at Chattanooga were used to create a simulation of 5,000,000 steps. This simulation will help imitate how the complex will move around in a solution box. All simulations were run at a

constant temperature of 303.15 K and a constant pressure of 1 atm. NAMD is a molecular dynamics code that is used to create high performing simulations [25]. NAMD will then use a visualization software called Visual Molecular Dynamics (VMD) which is used to obtain images and RMSD charts needed for the analysis.

IV. Results

The results from the SPR machine are graphed in the form of a sensorgram which plots the response against time. From the sensorgram, the equilibrium constant (K_D) can be obtained, and it will help determine how good the aptamer-protein affinity is. K_D is the rate at which association and dissociation are equal to each other or when the rate of protein attachment and detachment to the aptamer are equal [33]. The K_D value needs to be 10^{-9} or lower for the complex to have good affinity. As seen in Figure 1. the table shows that the K_D value from the SPR machine came out to be 1.105 x 10^{-8}. The K_D value is close to the required value for good affinity, so it was chosen for further studies. Now, the RMSD and energy charts of the different aptamer-protein conformations need to be analyzed.

Each frame in the simulation translates to 10 nano seconds. The following table shows the average values of the RMSD charts and the energies for each of the aptamer protein complexes.

Table 1. Average RMSD and energy values

Aptamer number	Average RMSD (Å)	Average Energy (kcal/mol)
1	3.776	-407,250
2	4.072	-372,875
3*	2.457	-433,125
4	3.916	-341,625
5	3.042	-562,750
6	2.803	-419,625
7	3.552	-372,250
8	3.552	-372187
9	3.724	-407,375
10	4.204	-408,000

*This complex was only able to be simulated for 4.5 nanoseconds.

Based on the average RMSD values, the sixth conformation would be the best and then the fifth conformation coming next since they have the lowest RMSD values. However, according to the average energy values the fifth conformation has the highest bond stability and then the sixth conformation is the second best. To choose between the two conformations, the RMSD charts should be analyzed for the least amount of fluctuation. The RMSD chart for complex six has less overall fluctuation as compared to complex five. Therefore, complex six would be the best one to choose for future studies.

V. Discussion

In the future, different types of surface proteins can be used as a means of targeting viruses and their SPR data should be studied to see which protein has the best affinity to an aptamer. Additionally, longer simulation times can be run to get better RMSD and energy values. It is not certain that the complex chosen is the best overall because its binding strength can reduce overtime. At the same time, another complex could have increasing values which indicates that it would be a better choice. From there, in vitro testing should be done to see how stable the complex is in a solution that mimics the inside of a human body. This allows researchers to know what the ideal environmental condition of the complex is, how long the complex can stay intact, how the complex deals with interference from the environment, how fast can the complex get to its target, etc.

VI. Limitations

The biggest limitation for this study was the simulation run time. The simulation should have been run for longer time in order to capture the RMSD value at which the complex is stable in the solution box. If the data was taken during longer time periods, the charts would be more reliable. Another limitation would be the lack of testing different proteins to act as targets. As shown, there are several different types of surface proteins that are abundant in SARS2. If more SPR analysis was done, there could be confirmation that the N protein is the best to use out of all the surface proteins.

VII. References

[1] Weiss, Susan R, and Julian L. Leibowitz. Coronavirus Pathogenesis - Sciencedirect. *ScienceDirect*. 2011. www.sciencedirect.com/science/article/pii/B9780123858856000092.

[2] Cui J, Li F, Shi ZL. Origin and evolution of pathogenic coronaviruses. Nat Rev Microbiol. 2019 Mar;17(3):181-192. doi: 10.1038/s41579-018-0118-9. PMID: 30531947; PMCID: PMC7097006.

[3] Pang X, Zhu Z, Xu F, et al. Evaluation of control measures implemented in the severe acute respiratory syndrome outbreak in Beijing. 2003. *JAMA.* 2003;290(24):3215–3221. doi:10.1001/jama.290.24.3215.

[4] Yang Y, Peng F, et al. The deadly coronaviruses: The 2003 SARS pandemic and the 2020 novel coronavirus epidemic in China. Journal of Autoimmunity. vol 109. May 2020. doi:10.1016/j.jaut.2020.102434.

[5] Berger A, Drosten Ch, et al. Severe acute respiratory syndrome (SARS) – paradigm of an emerging viral infection. Journal of Clinical Virology. vol 29. Jan 2004. doi:10.1016/j.jcv.2003.09.01.

[6] Smith Rogers, Lindsay. Origins of SARS-COV-2. *Johns Hopkins Bloomberg School of Public Health*, 15 Aug. 2022, publichealth.jhu.edu/2022/origins-of-sars-cov-2.

[7] Wu D, Wu T, et al. The SARS-CoV-2 outbreak: What we know. Int J Infect Dis. 2020 May;94:44-48. doi: 10.1016/j.ijid.2020.03.004. Epub 2020 Mar 12. PMID: 32171952; PMCID: PMC7102543.

[8] Yang Y, Xiao Z, et al. SARS-CoV-2: characteristics and current advances in research. Virol J. 2020 Jul 29;17(1):117. doi: 10.1186/s12985-020-01369-z. PMID: 32727485; PMCID: PMC7387805.

[9] Mullins E, Hudak ML, et al. PAN-COVID investigators and the National Perinatal COVID-19 Registry Study Group. Pregnancy and neonatal outcomes of COVID-19: coreporting of common outcomes from PAN-COVID and AAP-SONPM registries. Ultrasound Obstet Gynecol. 2021 Apr;57(4):573-581. doi: 10.1002/uog.23619. PMID: 33620113; PMCID: PMC8014713.

[10] "Covid-19 Map." *Johns Hopkins Coronavirus Resource Center*, coronavirus.jhu.edu/map.html.

[11] Acheson, N H. *Fundamentals of Molecular Virology.* John Wiley & Sons, Inc., 2007.

[12] Bakkers MJ, Lang Y, et al. Betacoronavirus Adaptation to Humans Involved Progressive Loss of Hemagglutinin-Esterase Lectin Activity. Cell Host Microbe. 2017 Mar

8;21(3):356-366. doi: 10.1016/j.chom.2017.02.008. PMID: 28279346; PMCID: PMC7104930.

[13] Satarker S, Nampoothiri M. Structural Proteins in Severe Acute Respiratory Syndrome Coronavirus-2. Arch Med Res. 2020 Aug;51(6):482-491. doi: 10.1016/j.arcmed.2020.05.012. Epub 2020 May 25. PMID: 32493627; PMCID: PMC7247499.

[14] Morse M, Sefcikova J, Rouzina I, Beuning PJ, Williams MC. Structural domains of SARS-CoV-2 nucleocapsid protein coordinate to compact long nucleic acid substrates. Nucleic Acids Res. 2023 Jan 11;51(1):290-303. doi: 10.1093/nar/gkac1179. PMID: 36533523; PMCID: PMC9841419.

[15] Sanjuán R, Domingo-Calap P. Mechanisms of viral mutation. Cell Mol Life Sci. 2016 Dec;73(23):4433-4448. doi: 10.1007/s00018-016-2299-6. Epub 2016 Jul 8. PMID: 27392606; PMCID: PMC5075021.

[16] Ni X, Castanares M, Mukherjee A, Lupold SE. Nucleic acid aptamers: clinical applications and promising new horizons. Curr Med Chem. 2011;18(27):4206-14. doi: 10.2174/092986711797189600. PMID: 21838685; PMCID: PMC3260938.

[17] Ohuchi S. Cell-SELEX Technology. Biores Open Access. 2012 Dec;1(6):265-72. doi: 10.1089/biores.2012.0253. PMID: 23515081; PMCID: PMC3559206.

[18] Wu J, Zhu Y, Xue F, Mei Z, Yao L, Wang X, Zheng L, Liu J, Liu G, Peng C, Chen W. Recent trends in SELEX technique and its application to food safety monitoring. Mikrochim Acta. 2014 Apr;181(5-6):479-491. doi: 10.1007/s00604-013-1156-7. PMID: 25419005; PMCID: PMC4239545.

[19] Huang et al. "The Aptamers Generated from HepG2 Cells." *Science China Chemistry*, Science China Press, 5 Apr. 2017, https://link.springer.com/article/10.1007/s11426-016-0491-7.

[20] Sabbih, Godfred O et al. "Computational generation and characterization of IsdA-binding aptamers with single-molecule FRET analysis." *Biotechnology journal* vol. 18,12 (2023): e2300076. doi:10.1002/biot.202300076.

[21] Nguyen HH, Park J, Kang S, Kim M. Surface plasmon resonance: a versatile technique for biosensor applications. Sensors (Basel). 2015 May 5;15(5):10481-510. doi: 10.3390/s150510481. PMID: 25951336; PMCID: PMC4481982.

[22] "Surface Plasmon Resonance (SPR)." *Cytiva,* www.cytivalifesciences.com/en/us/solutions/protein-research/knowledge-center/surface-plasmon-resonance/surface-plasmon-resonance.

[23] Chushak, Y.G., Martin, J.A., Chávez, J.L., Kelley-Loughnane, N., Stone, M.O. (2014). Computational Design of RNA Libraries for In Vitro Selection of Aptamers. In: Ogawa, A. (eds) Artificial Riboswitches. Methods in Molecular Biology, vol 1111. Humana Press, Totowa, NJ. https://doi.org/10.1007/978-1-62703-755-6_1

[24] Muppirala, U.K., Honavar, V.G. & Dobbs, D. Predicting RNA-Protein Interactions Using Only Sequence Information. *BMC Bioinformatics* **12**, 489 (2011). https://doi.org/10.1186/1471-2105-12-489

[25] Phillips JC, Braun R, Wang W, Gumbart J, Tajkhorshid E, Villa E, Chipot C, Skeel RD, Kalé L, Schulten K. Scalable molecular dynamics with NAMD. J Comput Chem. 2005 Dec;26(16):1781-802. doi: 10.1002/jcc.20289. PMID: 16222654; PMCID: PMC2486339.

[26] "Machine Learning: A Brief Introduction to Random Forest." *Albert Einstein College of Medicine*, einsteinmed.edu/uploadedfiles/centers/ictr/new/intro-to-random-forest.pdf.

[27] "What Is Support Vector Machine?" *IBM*, 12 Dec. 2023, www.ibm.com/topics/support-vector-machine.

[28] Kausar S, Said Khan F, Ishaq Mujeeb Ur Rehman M, Akram M, Riaz M, Rasool G, Hamid Khan A, Saleem I, Shamim S, Malik A. A review: Mechanism of action of antiviral drugs. Int J Immunopathol Pharmacol. 2021 Jan-Dec;35:20587384211002621. doi: 10.1177/20587384211002621. PMID: 33726557; PMCID: PMC7975490.

[29] https://www.webmd.com/covid/antivirals-covid-19

[30] https://clinicalcenter.nih.gov/blooddonor/donationtypes/convalescent_plasma.html

[31] "Targeted Protein Degradation using Proteolysis-Targeting Cimeras." *Thermo Fisher Scientific - US*, https://www.thermofisher.com/us/en/home/life-science/cell-analysis/cell-analysis-learning-center/protein-degradation-resource-center/targeted-protein-degradation-using-proteolysis-targeted-chimeras.html#:~:text=PROteolysis%20TArgeting%20Chimeras%20(PROTACs%C2%AE,to%20the%20proteasome%20for%20degradation.

[32] "Protein Degradation Using the Ubiquitin-Proteasome Pathway." *Thermo Fisher Scientific - US*, www.thermofisher.com/us/en/home/life-science/cell-analysis/cell-analysis-learning-center/protein-degradation-resource-center/protein-degradation-using-ubiquitin-proteasome-pathway.html.

[33] "Protein Interaction Analysis." *Bio-Rad*, www.bio-rad.com/webroot/web/pdf/lsr/literature/Bulletin_6044A.pdf.

VIII. Appendix

Figure 1. SPR report table

Report table

Curve	ka (1/Ms)	kd (1/s)	KD (M)	Rmax (RU)	Conc (M)	tc	Flow (ul/min)	kt (RU/Ms)	RI (RU)	Chi² (RU²)	U-value
	5.919E+10	654.0	1.105E-8	1.456E+4		1.559E+9				6.81E+5	95
Cycle: 8 1 nM					1.000E-9		30.00	4.845E+9	1220		
Cycle: 9 4 nM					4.000E-9		30.00	4.845E+9	1063		
Cycle: 10 8 nM					8.000E-9		30.00	4.845E+9	2043		
Cycle: 11 16 nM					1.600E-8		30.00	4.845E+9	2953		
Cycle: 12 32 nM					3.200E-8		30.00	4.845E+9	3783		

Figure 2. SPR sensorgram

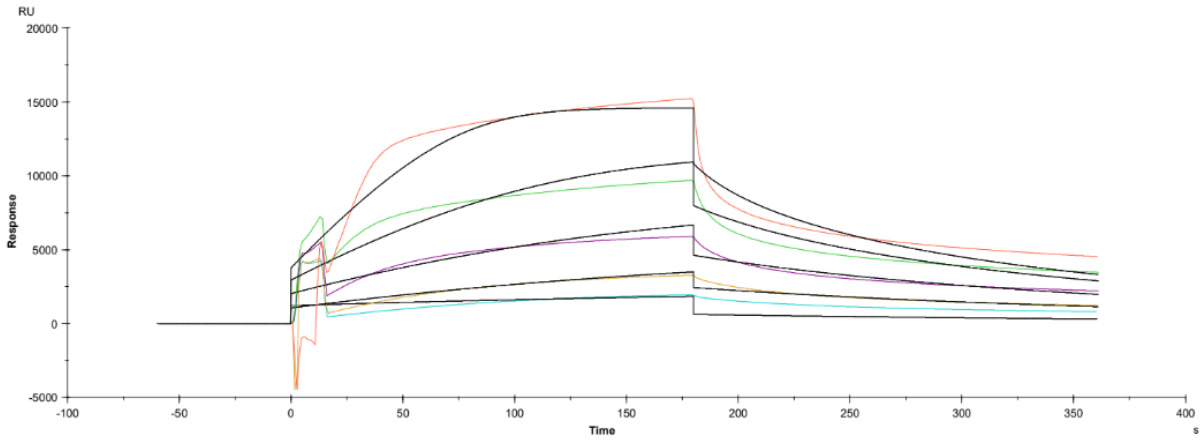

Figure 3. Aptamer-protein conformation 1

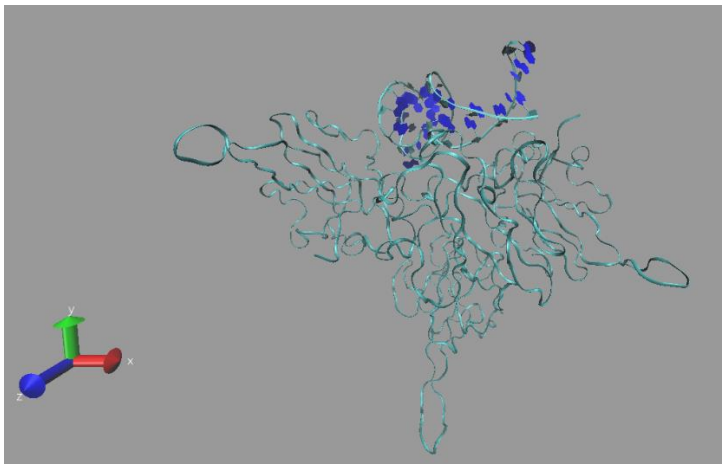

Figure 4. Aptamer – protein conformation 2

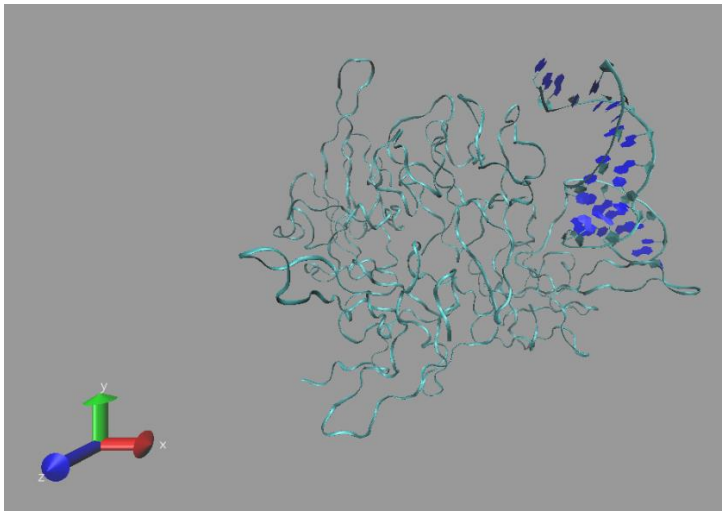

Figure 5. Aptamer – protein conformation 3

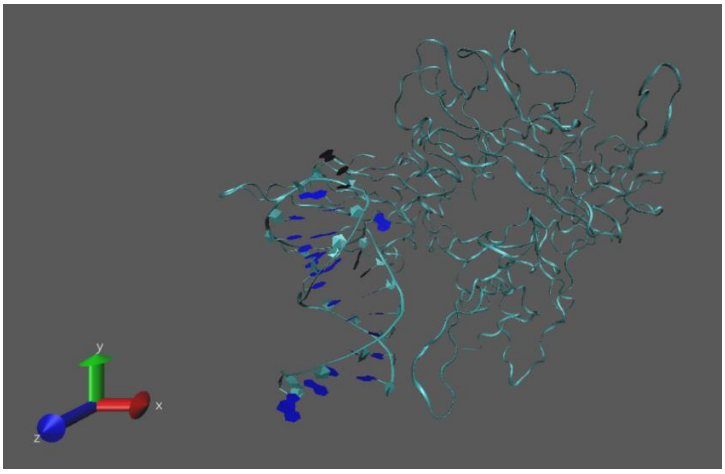

Figure 6. Aptamer – protein conformation 4

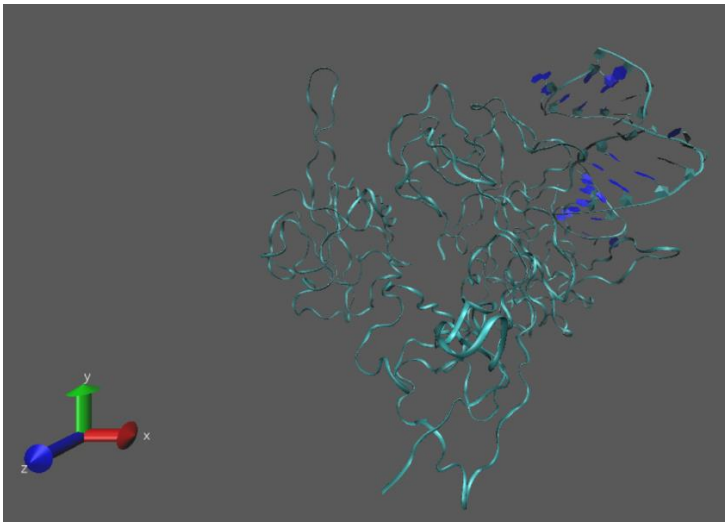

Figure 7. Aptamer – protein conformation 5

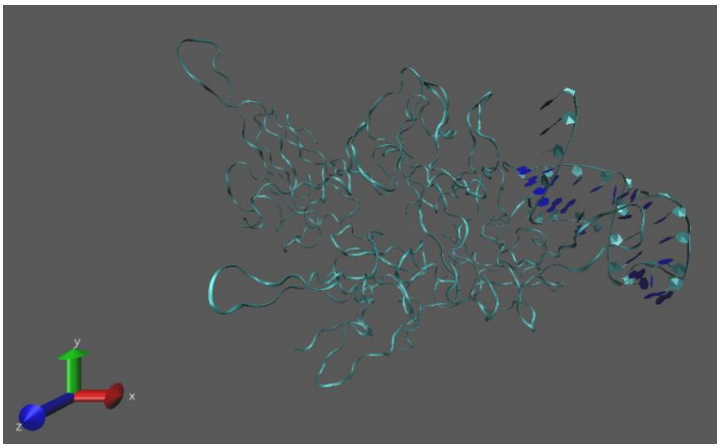

Figure 8. Aptamer – protein conformation 6

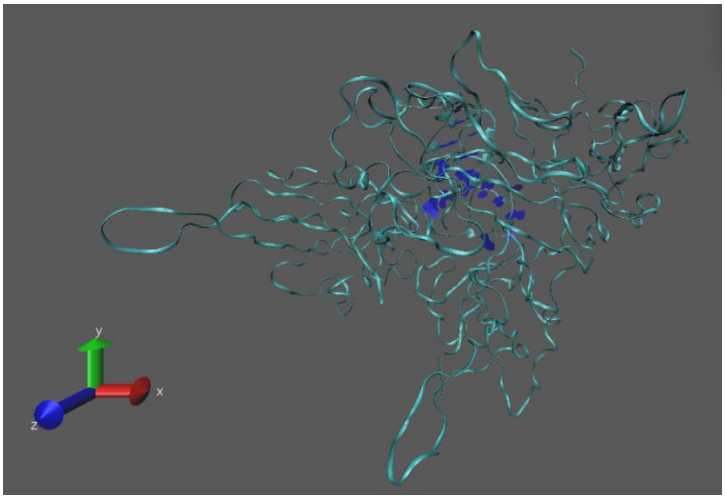

Figure 9. Aptamer – protein conformation 7

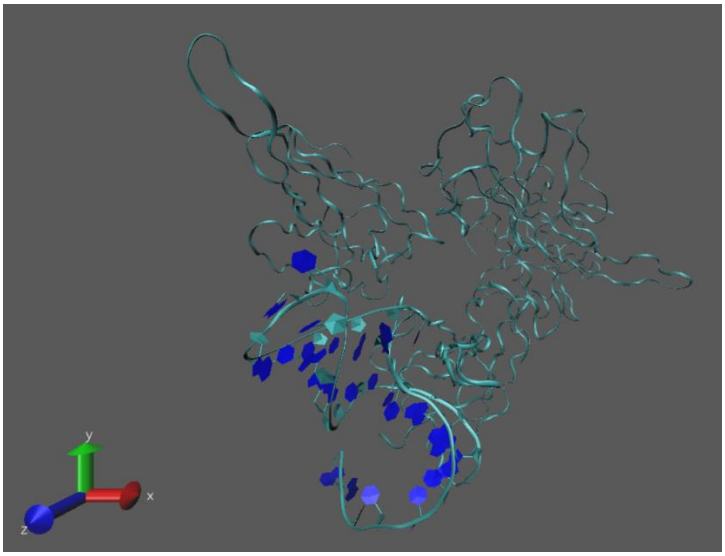

Figure 10. Aptamer – protein conformation 8

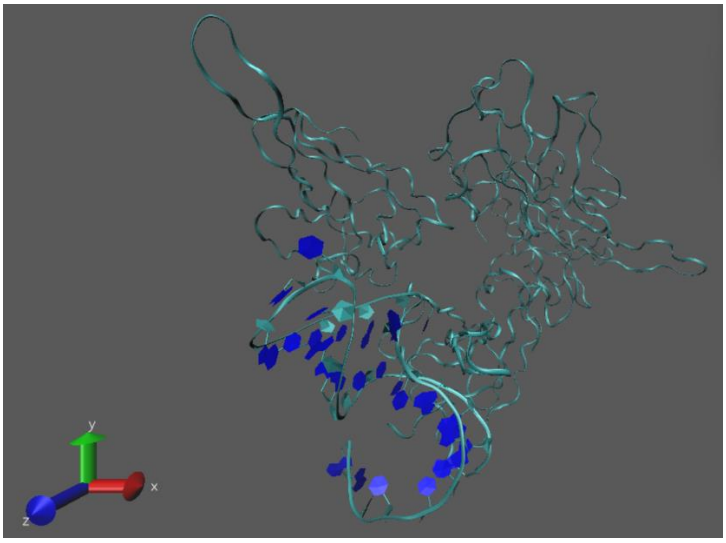

Figure 11. Aptamer – protein conformation 9

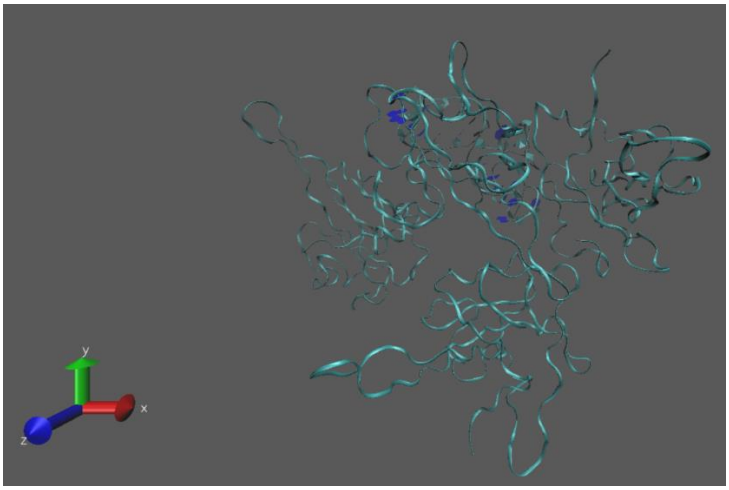

Figure 12. Aptamer – protein conformation 10

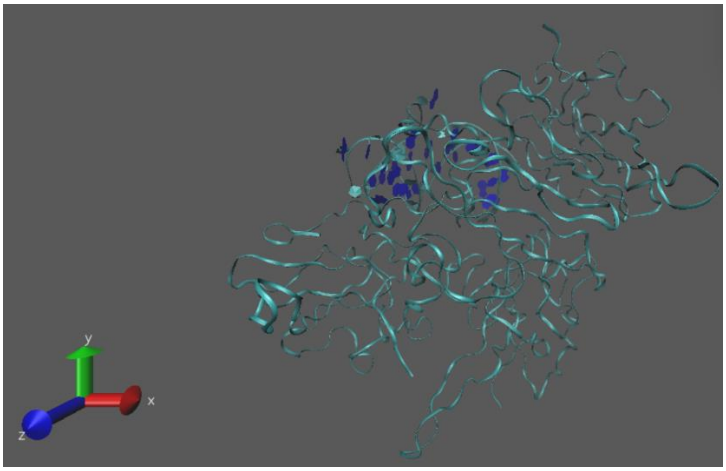

Figure 13. Complex 1 RMSD chart

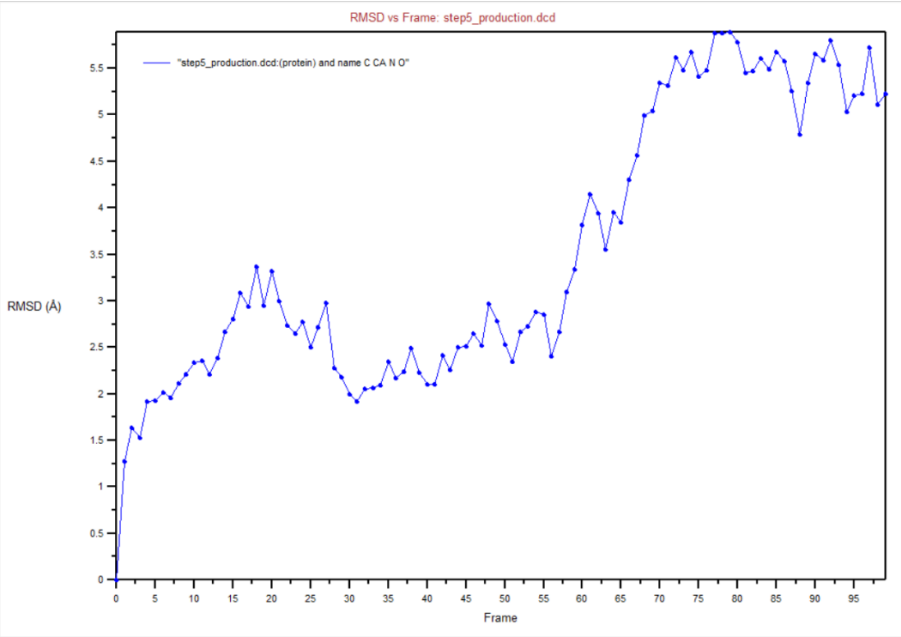

Figure 14. Complex 2 RMSD chart

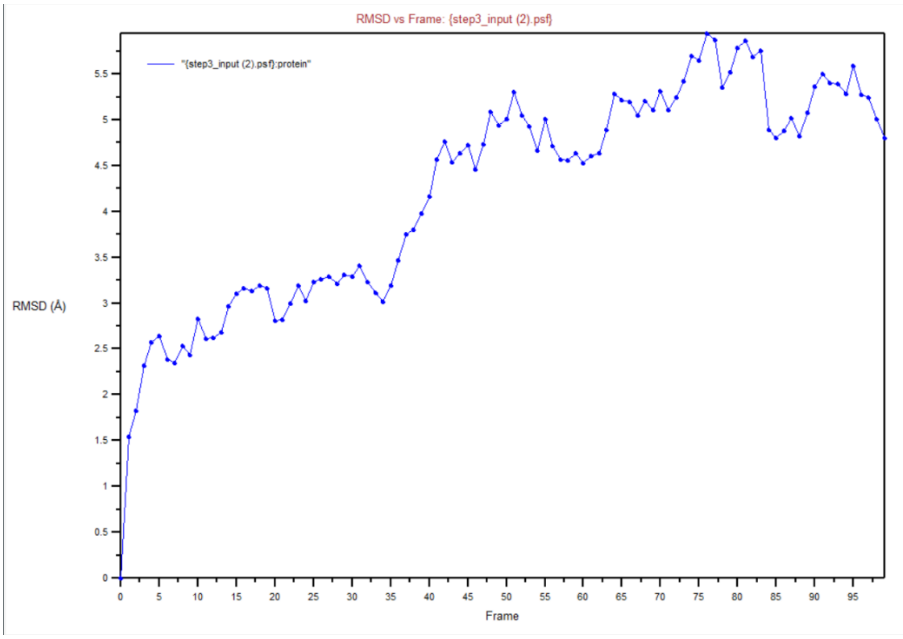

Figure 15. Complex 3 RMSD chart

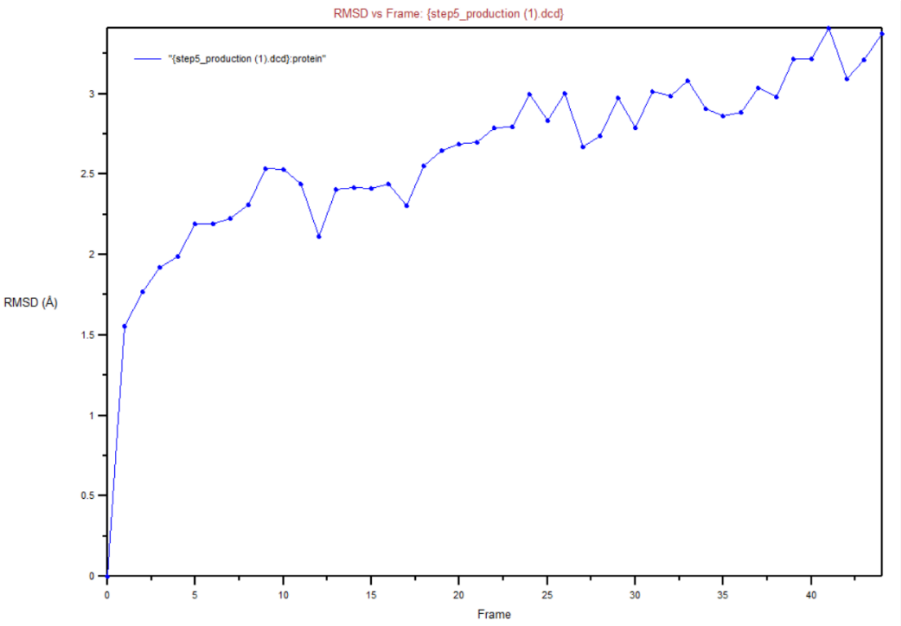

Figure 16. Complex 4 RMSD chart

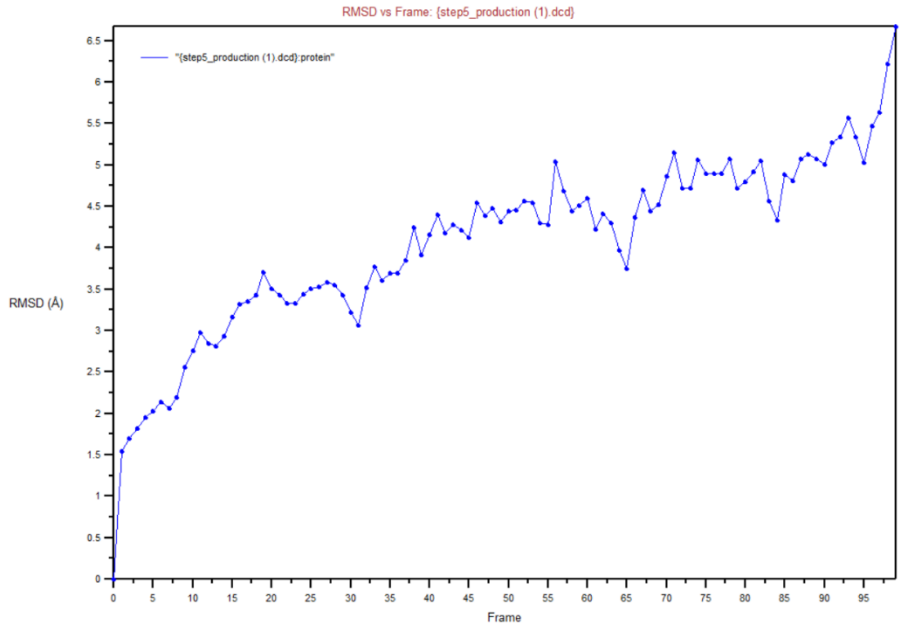

Figure 17. Complex 5 RMSD chart

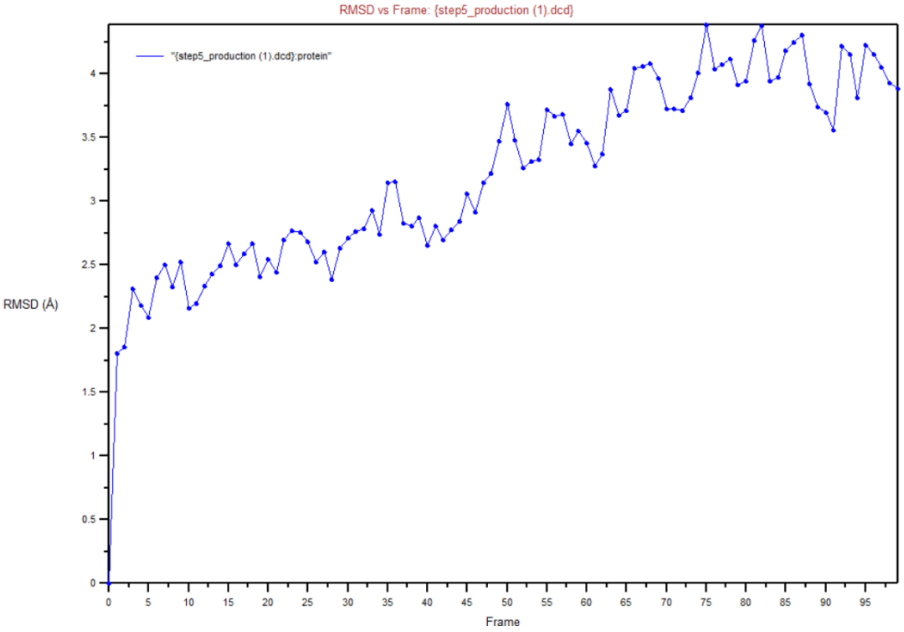

Figure 18. Complex 6 RMSD chart

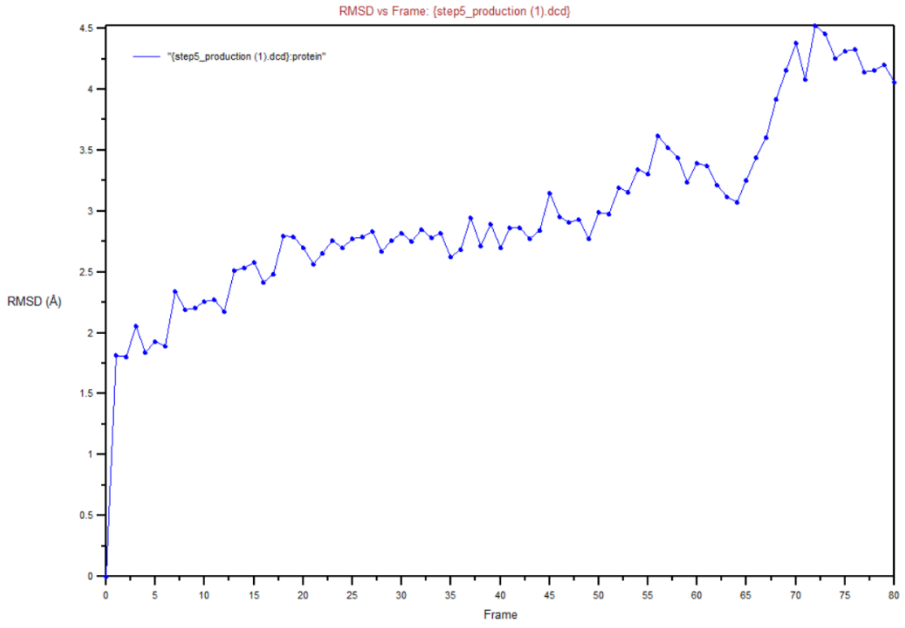

Figure 18. Complex 7 RMSD chart

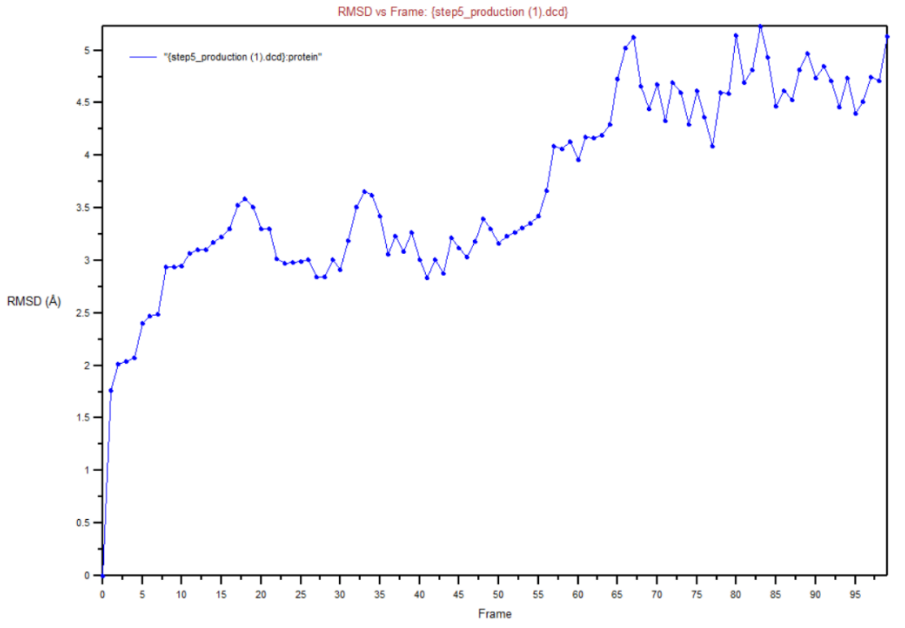

Figure 19. Complex 8 RMSD chart

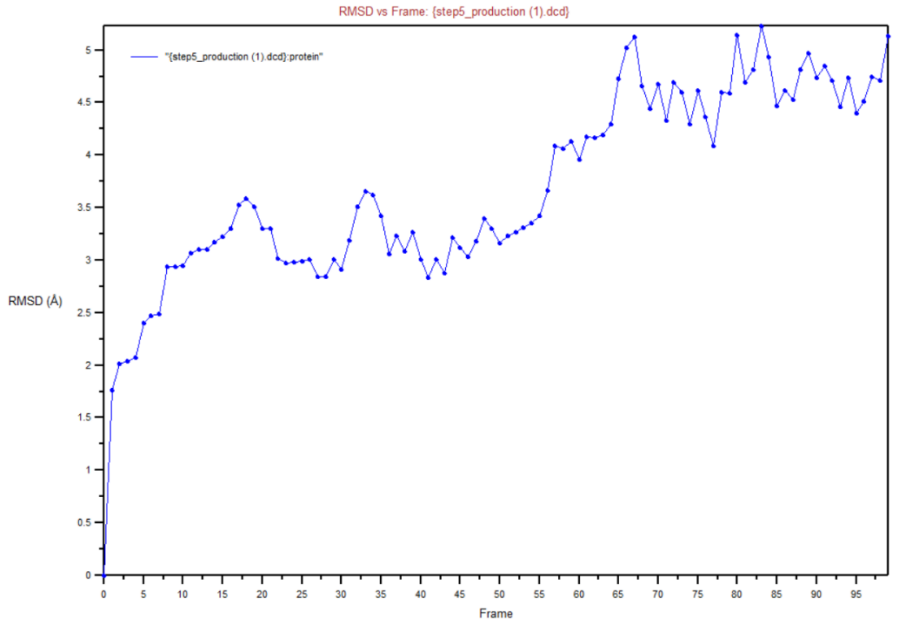

Figure 20. Complex 9 RMSD chart

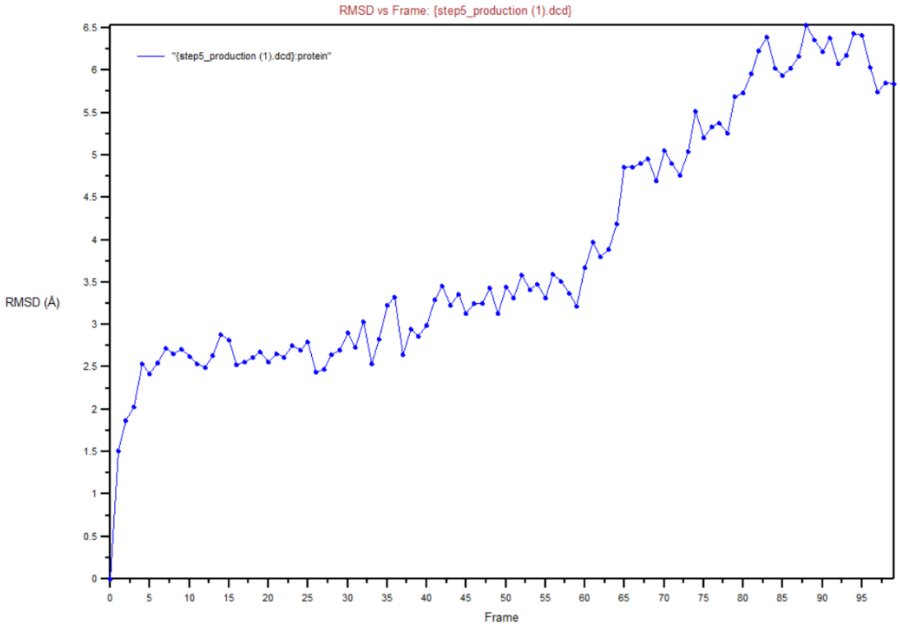

Figure 21. Complex 10 RMSD chart

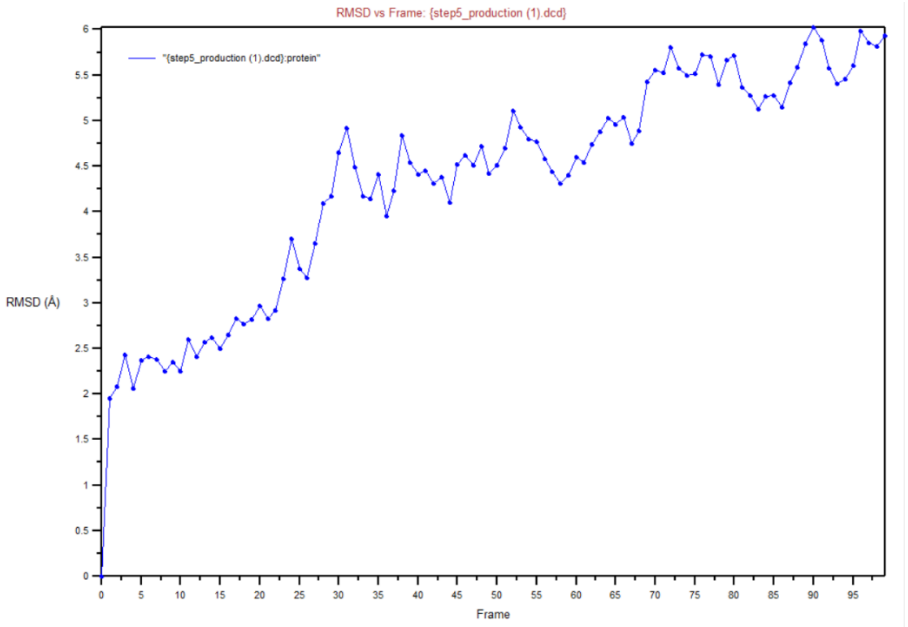

Figure 22. Complex 1 energy chart

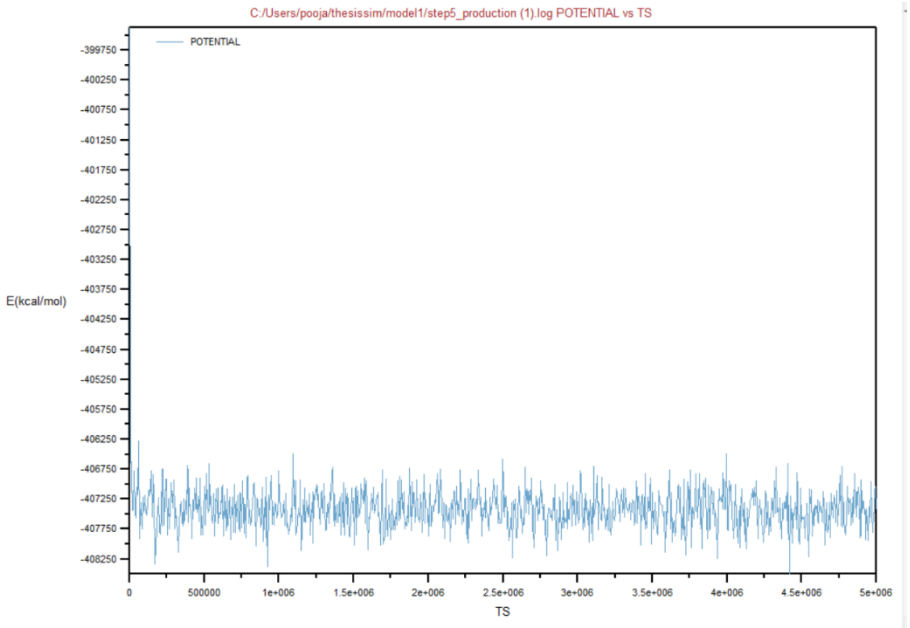

Figure 23. Complex 2 energy chart

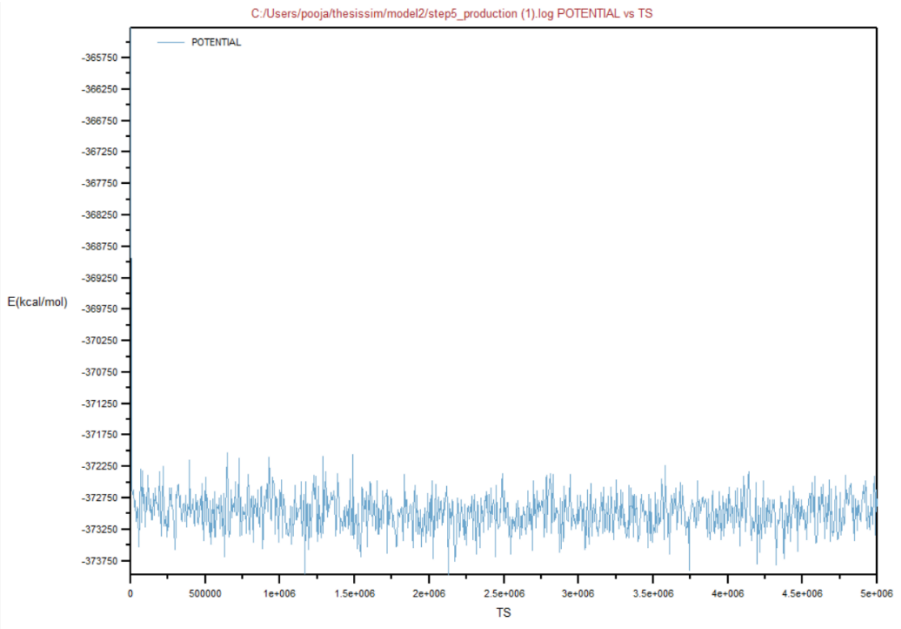

Figure 24. Complex 3 energy chart

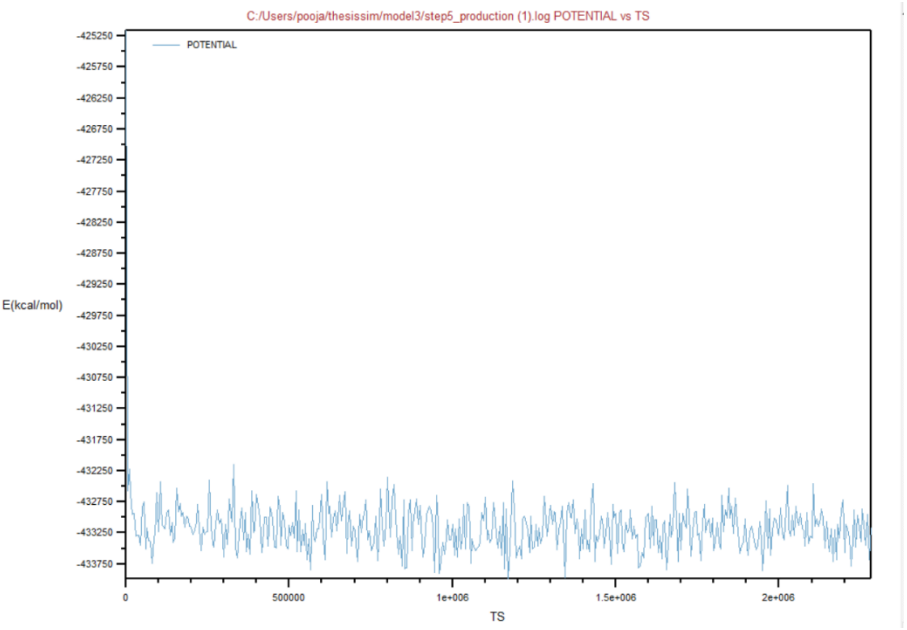

Figure 25. Complex 4 energy chart

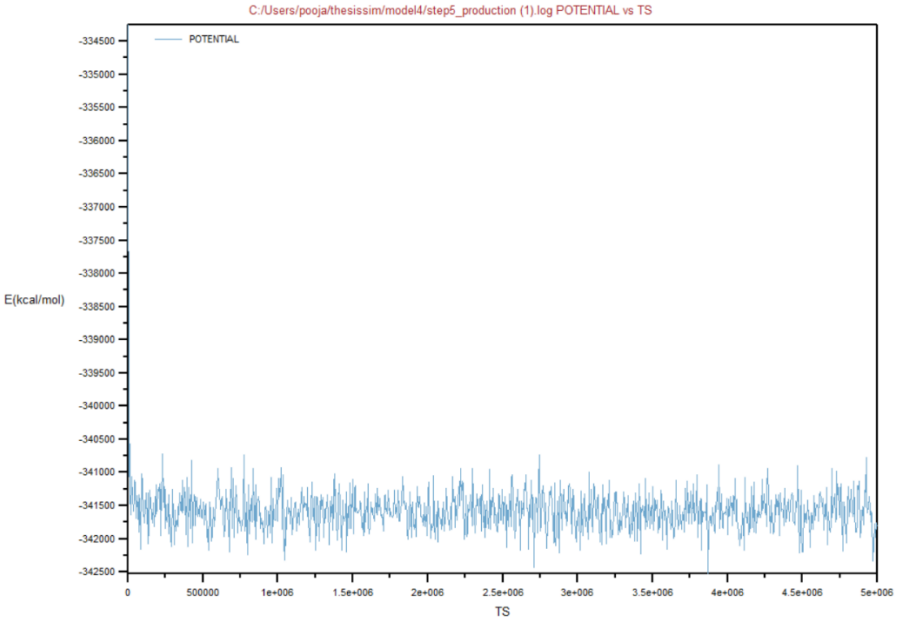

Figure 26. Complex 5 energy chart

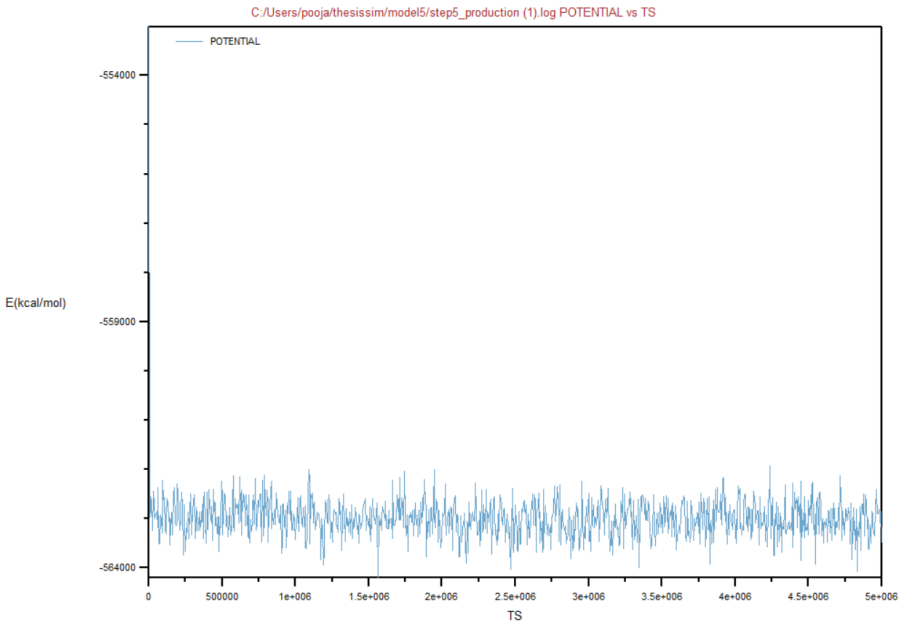

Figure 27. Complex 6 energy chart

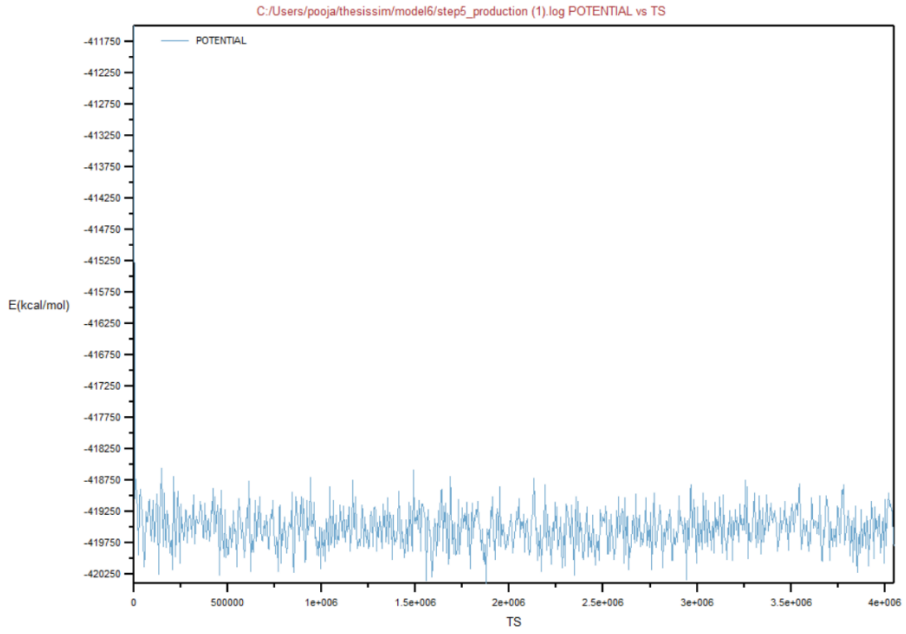

Figure 28. Complex 7 energy chart

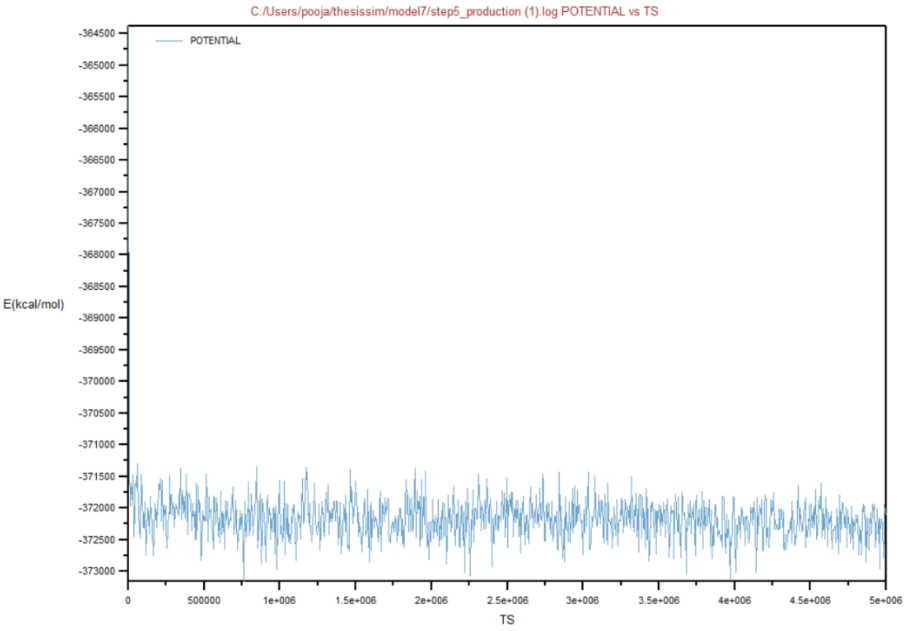

Figure 29. Complex 8 energy chart

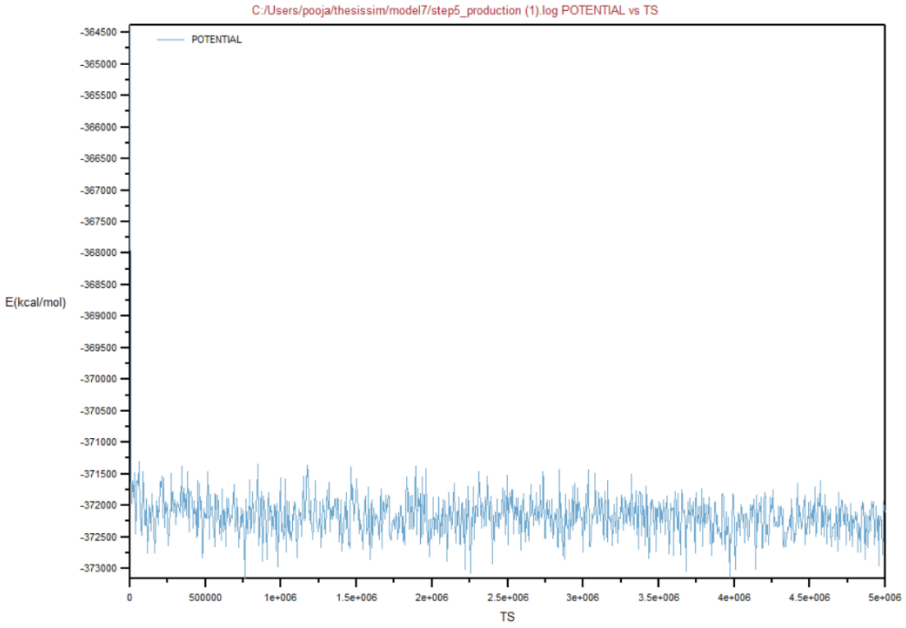

Figure 30. Complex 9 energy chart

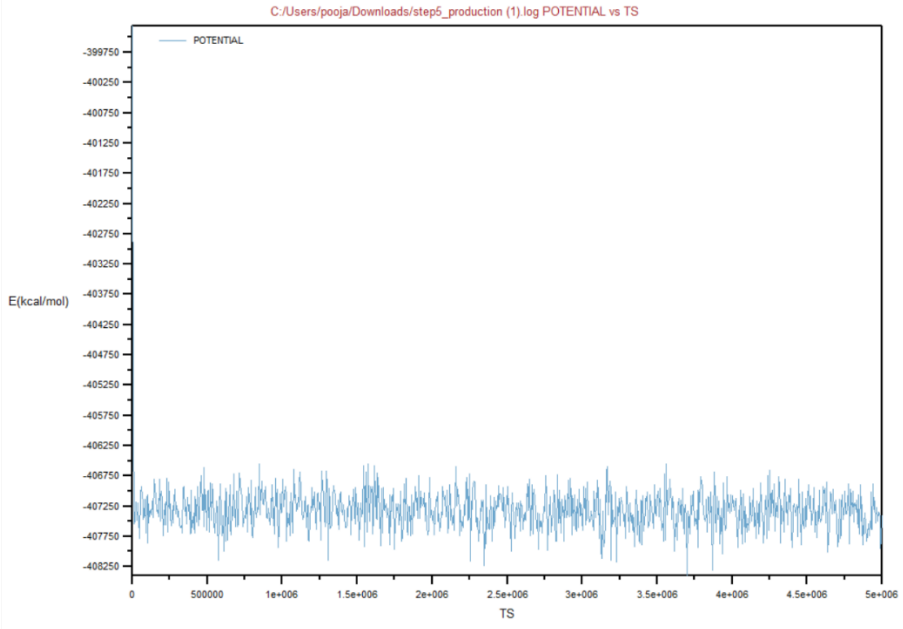

Figure 31. Complex 10 energy chart